

Research paper

SPF-Net: Solar panel fault detection using U-Net based deep learning image classification



Rifat Al Mamun Rudro ^a, Kamruddin Nur ^a, Md. Faruk Abdullah Al Sohan ^a, M.F. Mridha ^{a,*}, Sultan Alfarhood ^b, Mejdl Safran ^b, Karthick Kanagarathinam ^c

^a Department of Computer Science, American International University-Bangladesh, Dhaka, Bangladesh

^b Department of Computer Science, College of Computer and Information Sciences, King Saud University, Riyadh 11543, Saudi Arabia

^c Department of Electrical and Electronics Engineering, GMR Institute of Technology, Rajam, India

ARTICLE INFO

Keywords:
Fault detection
Inceptionv3
VGG16
Segmentation
U-Net
Solar panel

ABSTRACT

The detection of faults in solar panels is essential for generating increased amounts of renewable green energy. Solar panels degrade over time due to physical damage, dust, or other faults. Numerous studies have been conducted to detect and monitor solar panel faults in real-time. This research examines the deployment of deep learning models for identifying these faults. In this research, we propose a novel deep learning model combining the InceptionV3-Net with U-Net architecture. The proposed architecture applies the InceptionV3 base with ImageNet weights, enhanced by convolutional layers, squeeze-and-excitation (SE) blocks, residual connections, and global average pooling. The model includes two dense layers with LeakyReLU and batch normalization, ending with a Soft-Max output layer. Incorporating image segmentation into deep learning models significantly improves the precision and test accuracy of identifying issues in solar panels. The proposed model achieves exceptional performance, having a validation accuracy of 98.34%, a test accuracy of 94.35% with an F1 score of 0.94, a precision of 0.94, and a Recall of 0.94.

1. Introduction

The global energy landscape has significantly transitioned toward ecologically friendly and sustainable power-producing systems. Solar power systems have emerged as a crucial contribution to this change process. In addition to providing economic and environmental advantages, solar panel devices can capture atmospheric sunlight and transform it into electrical power. These factors include growing public awareness of environmental issues, the desire for energy independence, incentives for economic expansion, and the scalability inherent in solar technology. In today's energy industry, multiple factors contribute to the growth of solar power installations (Li et al., 2024). It is becoming more common for developed and developing countries to deploy substantial solar power systems (Li et al., 2023). When it comes to boosting energy production, lowering operating costs, and ensuring the long-term sustainability of these advancements, the proper management and maintenance of solar panels inside these power plants is very necessary. It is hard to emphasize the importance of having effective monitoring and cleaning methods for solar energy systems. Solar power plants have attracted a lot of attention during this wave of transformation, regardless of whether they are located in developed countries

or developing ones (Liu et al., 2023). With the capacity to meet the electricity requirements of enormous populations, these enormous solar plants are well-positioned to play a crucial role in the future of energy generation.

The efficient operation and maintenance of solar panels inside these power plants are essential to maximizing energy production, reducing costs, and ensuring the long-term viability of these plants (Hu et al., 2016). Many causes, including dust buildup, snow cover, bird droppings, and electrical abnormalities on the surfaces of solar panels in Fig. 1, are responsible for energy losses. These losses highlight the effectiveness of monitoring and cleaning operations in solar power systems. This paper aims to find the utilization of deep learning model classifiers. Using Deep learning model classifiers can help optimize maintenance efforts and minimize energy losses by correctly finding and categorizing surface defects on solar panels in Fig. 2 (Ramaneti et al., 2021). This research can potentially increase the efficiency and stability of solar power systems. In recent years, research has focused on solar panel power plants, specifically in the areas of fault detection and power generation. Despite the clear advantages of photovoltaic (PV) systems, several challenges remain in maintaining the optimal performance of solar panels. Previous research has shown that existing deep

* Corresponding author.

E-mail addresses: rifat.rudro@aiub.edu (R.A.M. Rudro), kamruddin@aiub.edu (K. Nur), faruk.sohan@aiub.edu (M.F.A.A. Sohan), firoz.mridha@aiub.edu (M.F. Mridha), sultanf@ksu.edu.sa (S. Alfarhood), mejdl@ksu.edu.sa (M. Safran), karthick.k@gmrit.edu.in (K. Kanagarathinam).



Fig. 1. Dusty Solar Panel Installation in the rooftop.

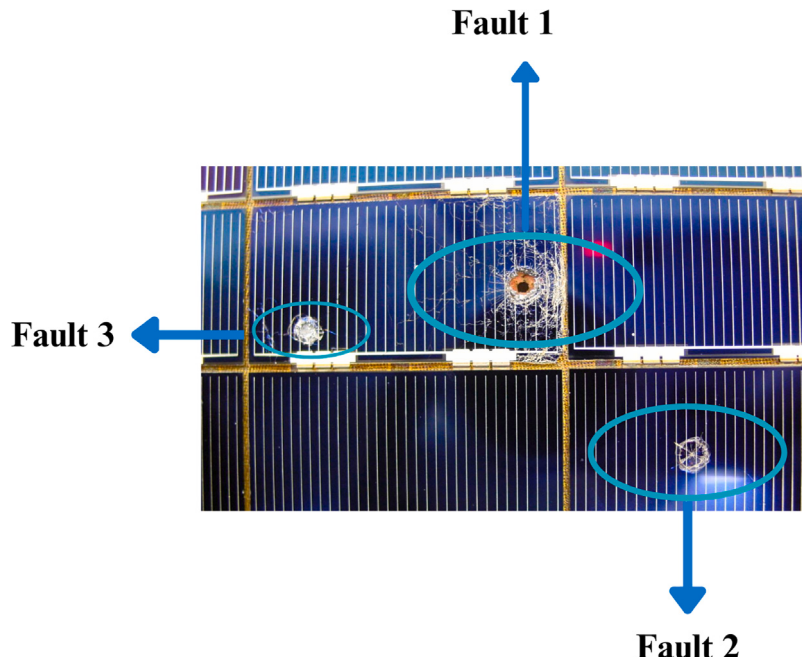


Fig. 2. Fault Finding in Solar Panel — **Fault 1** shows shattered glass and cell damage, **Fault 2** indicates a burnt area in the center of cells, and **Fault 3** highlights a fractured cell.

learning models for fault detection often struggle to accurately identify less common faults due to imbalanced datasets. Additionally, real-time conditions factors have limited previous research models. Despite significant progress in utilizing deep learning for solar panel fault detection, several research gaps have been identified. These gaps include issues with data quality and imbalance, adaptability to real-world settings, interpretability of results, coverage of fault types, implementation complexity and cost, handling data noise and complexity, achieving model precision, and generalization.

In the past several years, a significant worldwide movement in the energy sector has promoted using environmentally friendly and sustainable power-generating sources, including solar power (Sharma and Sharma, 2017). These systems convert the sun's plentiful energy into electrical energy, giving several environmental and economic benefits (Khan et al., 2023). The existing deep learning models for fault detection in solar panels often fail to accurately identify less common

faults due to imbalanced datasets. Additionally, current models do not perform well under real-world conditions such as varying lighting, weather, and physical obstructions. Our research addresses these issues by developing the InceptionV3-Net with U-Net Architecture. The proposed model enhances fault detection accuracy and efficiency, even under diverse conditions.

The proposed model's novelty lies in its efficient design, with the InceptionV3 base with ImageNet weights, convolutional layers, Squeeze-and-Excitation (SE) blocks, residual connections, and global average pooling. Additionally, the model includes two dense layers with LeakyReLU and batch normalization, culminating in a Soft-Max output layer. This combination of architectural elements enables the model to effectively capture features at various scales and identify faults in solar panels.

The research objective is broad and includes numerous significant points:

- **Panel Fault Detection:** To establish a system that can identify various impurities, such as dust, snow, bird droppings, physical damage, and electrical issues, that frequently harm solar panel surfaces.
- **Improvement of precision:** To achieve high precision while identifying impurities. Select classifiers will require optimization and fine-tuning, and feature engineering and selection techniques will require research to improve their performance to verify the system.
- **Efficiency Improvement:** Enhance the tracking system's efficiency by accurately identifying the need for cleaning or repairs, thereby boosting energy production efficiency.
- **Cost Reduction:** Reduce maintenance costs through efficient monitoring and cleaning strategies, minimizing manual inspections and repairs.
- **Resource Conservation:** Align with sustainability goals by minimizing resource use in solar panel maintenance, cleaning, and repair only when necessary.

The current energy sector presents an excellent opportunity for the development of solar power plants (Snegirev et al., 2017). Both developed and developing countries are swiftly adopting extensive solar power installations. Efficiently managing and maintaining solar panels in power plants is crucial for optimizing energy production, minimizing operational expenses, and guaranteeing the enduring viability of these developments (Durany, 2023). The presence of dust, snow, bird droppings, and other physical and electrical problems on the surfaces of the solar panels may lead to energy losses (Ou-Yang and Ren, 2009). The need for efficient monitoring and cleansing protocols in solar energy systems cannot be emphasized enough (García et al., 2022). Based on that purpose, we have selected research subjects to enhance the image processing and classification tasks related to various types of damage to solar panels.

The subsequent sections of the paper are structured in the following manner: Section 2 provides the preceding related works. With numerous figures and facts, Section 3 provides a thorough description of the methodology. The proposed model is explained in Section 4 with some figures and equations, while Section 5 provides a brief description of the evaluation matrix. The proposed model outcome is discussed in Section 6, while Section 9 serves as the paper's conclusion.

2. Related works

Deep learning has been used to detect solar faults, emphasizing choosing and training deep learning architectures to distinguish between working and damaged solar panels. Previously, several researchers used deep learning for solar fault recognition. Selecting a deep learning architecture and training the model to transform between working solar panels and those emphasizing not. They overcame a lot of problems, such as getting different types of well-labeled data, fixing problems with data imbalance (Alsaafseh et al., 2018a), making sure the model could be used for new types of faults, dealing with higher computational needs, and fixing issues with the model's ability to work with other models (Anon, 2021), on the detection of faults in solar panels. This involved finding the issues of collecting different data types, implementing remote monitoring systems, and utilizing machine learning to diagnose problems (Dhanraj et al., 2021). They also employ sensors to detect errors quickly. Some challenges they face include ensuring data quality, spotting errors, avoiding false positives and negatives, managing implementation costs, and extrapolating across different scenarios (Bemposta Rosende et al., 2020). These intricacies draw attention to the challenges faced by complex solar panel fault detection systems using these models.

To detect anomalies in PV panels, the study applies extreme gradient boosting (XGBoost), light gradient boosting (LGBM), and categorical boosting (CatBoost) using real-time temperature and irradiance

data (Adhya et al., 2022). LGBM did better than the other models, with a 99.996% precision with class balancing issues. The study encountered several difficulties, including possible problems with the quality of the data, limited coverage of fault types, concerns about generalizing the results, implementation complexity, limitations on specific sensors and hardware, difficulties interpreting the algorithms, and a lack of false positive (Pamungkas et al., 2023) and negative analysis. Developed methods for diagnosing PV array problems. The research article focuses on creating and evaluating classifiers based on deep learning algorithms to automatically identify and diagnose typical issues in photovoltaic arrays. They employed a variety of deep learning and machine learning models, including ImageNet, support vector machines, decision trees, and KNN, by using historical data (Badr et al., 2021).

PV array power production is developed and executed by innovative methods to enhance the reliability and efficiency of photovoltaic systems, with a particular focus on problem identification and diagnosis (Rao et al., 2019). Using the K-means approach, they achieved 99.72% model precision with data noise in their research, which has both complex data handling and implementation processes.

A convolutional neural network (CNN) and a fine-tuned visual geometry group (VGG-16) model to examine thermal images with less complexity for detection in their research (Kellil et al., 2023). When using class-balanced distributions and small-DCNN pre-trained models, the research achieved a precision of 99.91% for identification and 99.80% for recognizing five distinct types of error classifications. Using deep learning techniques to enhance issue diagnosis and maintenance, Naveen Venkatesh and Sugumaran (2021) has significantly improved defect identification in renewable energy. By utilizing critical features extracted from aerial images captured by UAVs and deep learning methods like CNNs and a pre-trained VGG16 network, they can classify several fault categories, such as burn marks, delamination, discoloration, glass breakage, good panel, and snail trail.

By using statistical hypothesis testing with machine learning, precisely Gaussian process regression (GPR), using a generalized likelihood ratio test (GLRT) chart (Fazai et al., 2019). They were validated using natural and simulated PV data, focusing on power, voltage, and current, which are three critical attributes of the system. An RMVDM can efficiently identify and localize using defects such as dust, micro-cracks, and spotlights. The model employs a multi-variant deep learning architecture to train and detect errors (Sridharan and Sugumaran, 2021). Before training, the image data is preprocessed using the Region-Based Histogram Approximation (RHA) method, and features are extracted using the Gray Scale Quantization Technique (GSQA) (Henry et al., 2020). The research article employs the higher-order texture localization (HOTL) technique and both defect class support (DCS) values to train and recognize faults precisely throughout the testing process.

Thermal image and deep learning for detecting environmental faults in solar panels. They modified Squeeze-Net as the best-pretrained CNN model by implementing trial and error. Using thermal images as training data. This algorithm can identify environmental problems. The results show that Squeeze-Net can find and classify issues with solar panels with better data quality and less data description, with a testing precision of 99.74% and an F1 score of 0.9818.

3. Methodology

The step by step procedure of the proposed framework is described in the following subsections and the framework architecture is depicted in Fig. 3.

3.1. Proposed framework

The objective of solar panel fault detection is to complete the methods in four stages. In the first stage, we focus on image collection. In this phase, we use advanced data preprocessing techniques to improve the data quality. We have collected high-resolution images of solar

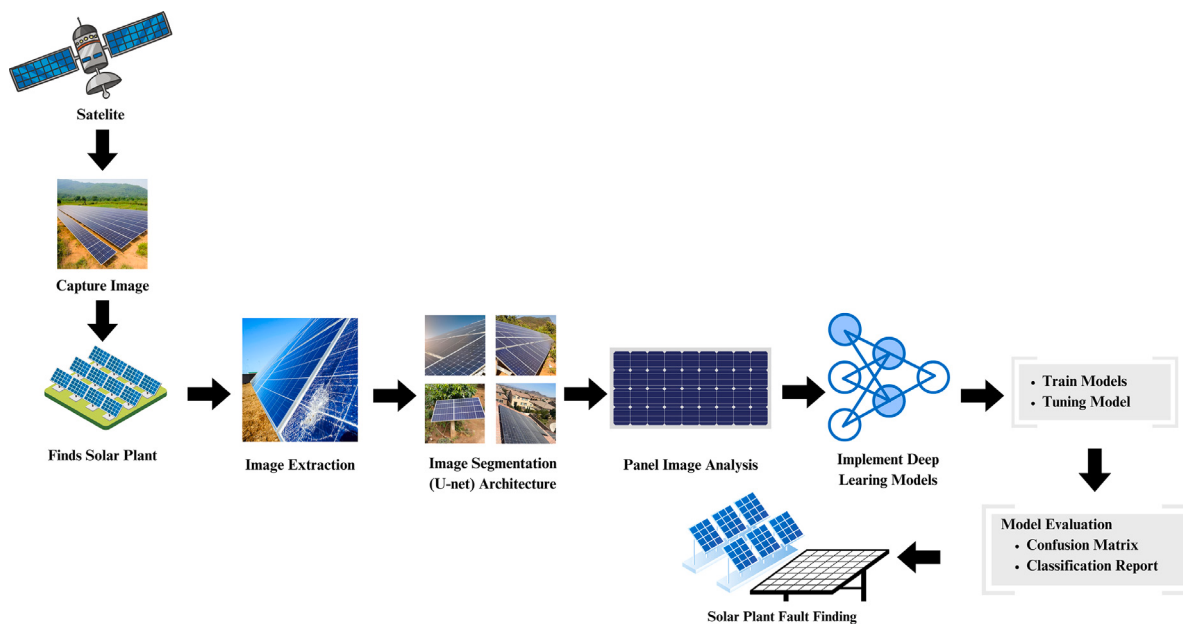


Fig. 3. Proposed Framework. Using Satellite Imagery, Image Segmentation, Deep Learning models, and Model Evaluation.

Table 1
Details of images in solar panel fault segmentation and classification dataset.

Dataset name	Total images
Segmentation Data	4616
Classification Data	885

Table 2
Distribution of images in different classes for segmentation.

Class name	Train	Validation	Test	Total image
Ground Cropland	1034	317	367	1718
Ground Grassland	133	53	48	234
Ground SalineAlkali	417	154	133	704
Ground Shrubwood	155	43	40	238
Ground WaterSurface	758	257	235	1250
Rooftop	272	99	100	471
Total	2769	923	923	4615

panels. The second phase is solar panel segmentation, using image processing U-Net algorithms to create masking. The next step is to build a comprehensive system for error categorization by identifying and categorizing issues using deep learning models. Based on the model results, we have analyzed the impact of power consumption.

3.2. Solar panel dataset

We have chosen and assessed two public-access datasets to verify the research approach. **Table 1** indicates the number of images in two distinct datasets: Segmentation Data and Classification Data. The images were split in a 60%-20%-20% ratio for training, validation, and testing, respectively, shown in **Table 2**. The Segmentation Data dataset includes 4616 images, with 2769 for training, 923 for validation, and 924 for testing. Conversely, the Classification Data dataset comprises 885 images, with 531 for training, 177 for validation, and 177 for testing. A vast array of photovoltaic (PV) samples from sources, including satellite and aerial photography (**Fig. 4**), make up the first dataset for the proposed framework (**Hou et al., 2021**).¹

Table 3
Distribution of images in different classes for training, validation, and testing in classification.

Class name	Train	Validation	Test	Total image
Physical-Damage	41	14	14	69
Electrical-damage	61	20	21	102
Snow-Covered	71	24	24	119
Clean	115	38	39	192
Dusty	113	38	37	188
Bird-drop	129	43	43	215
Total	531	177	177	885

The segmentation dataset contains six categories: ground cropland, grassland, saline-alkali, shrubwood, water-surface, and rooftop. These categories collectively represent the image distribution across different classes, as shown in **Fig. 5**.

The second dataset is required to examine how well various deep-learning image classifiers can recognize the surface conditions of solar panels. The dataset comprises six distinct categories: clean, dusty, bird drop, electrical damage, physical damage, and snow-covered. These categories collectively represent a spectrum of surface conditions frequently encountered in solar panel installations, as visually depicted in **Fig. 6**. These categories exhibit an inherent imbalance in their distribution within the dataset. These data sources validate the U-Net model architecture's image processing capacity and implement the proposed deep learning model. This evaluation process determines how accurate the U-Net model and proposed InceptionV3-Net for correctly finding and classifying anomalies in different surface conditions on solar panels (**Chen et al., 2023**).

The **Table 3** presents a breakdown of the images distributed among six distinct classes for a classification task. A 60:20:20, where the ratio divided in train:validation: test split is employed, resulting in 531 images for the training dataset, with varying training images for each class. By allocating images for training, validation, and testing, it is possible to evaluate the performance of the classification model.

3.3. Data pre-processing and augmentation

In the initial image processing stage, the images are cropped to dimensions of 256 × 256 pixels. The values are normalized by being

¹ <https://zenodo.org/records/5171712>

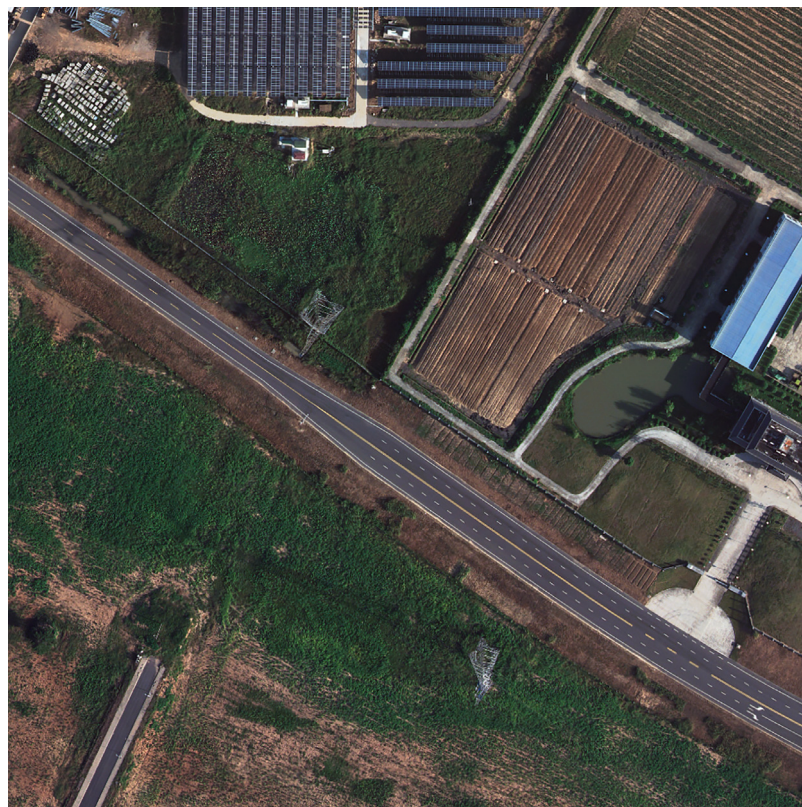


Fig. 4. Satellite view of a solar plant adjacent to agricultural fields and a road, image collected from public data sources.

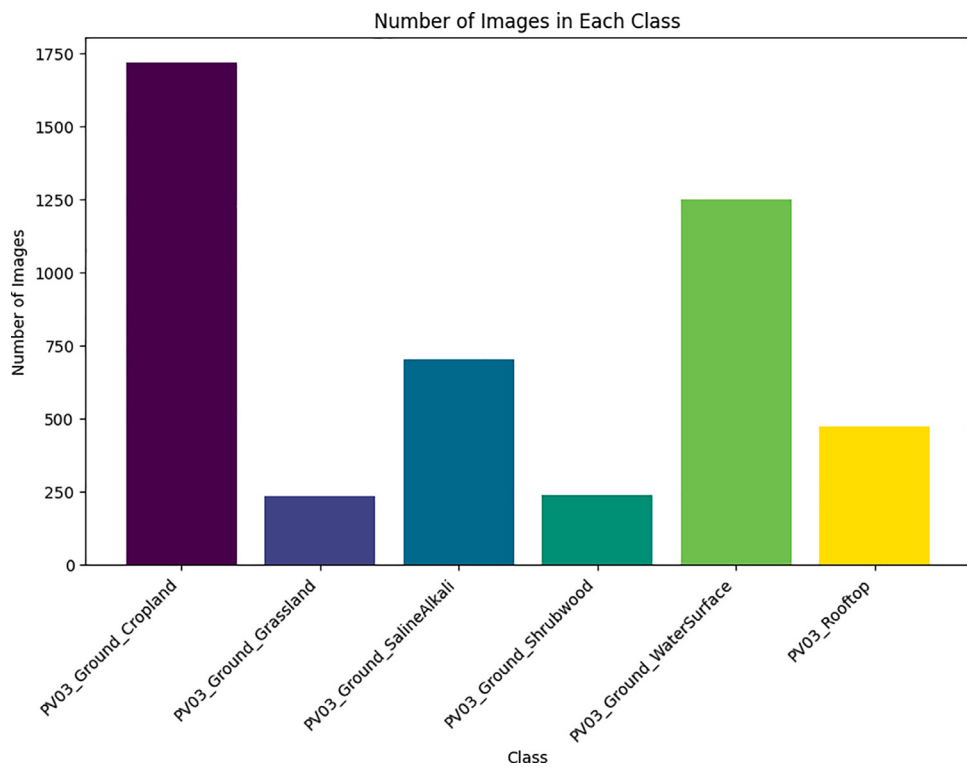


Fig. 5. The graph shows the distribution of images across different classes. Specifically for ground cropland, grassland, saline/alkali land, shrub/woodland, water surface, and rooftop, as part of a dataset labeled PV03.

divided by 255-pixel units, resulting in a range of values between 0 and 1. In addition, binary masks (Alsafseh et al., 2018b) are generated from the masks as shown as Fig. 7. During data augmentation, there is

a 50% chance that input pictures and masks will be randomly inverted horizontally. The first dataset is then divided into training, validation, and testing sets, with a batch size of 24 sets used for training.

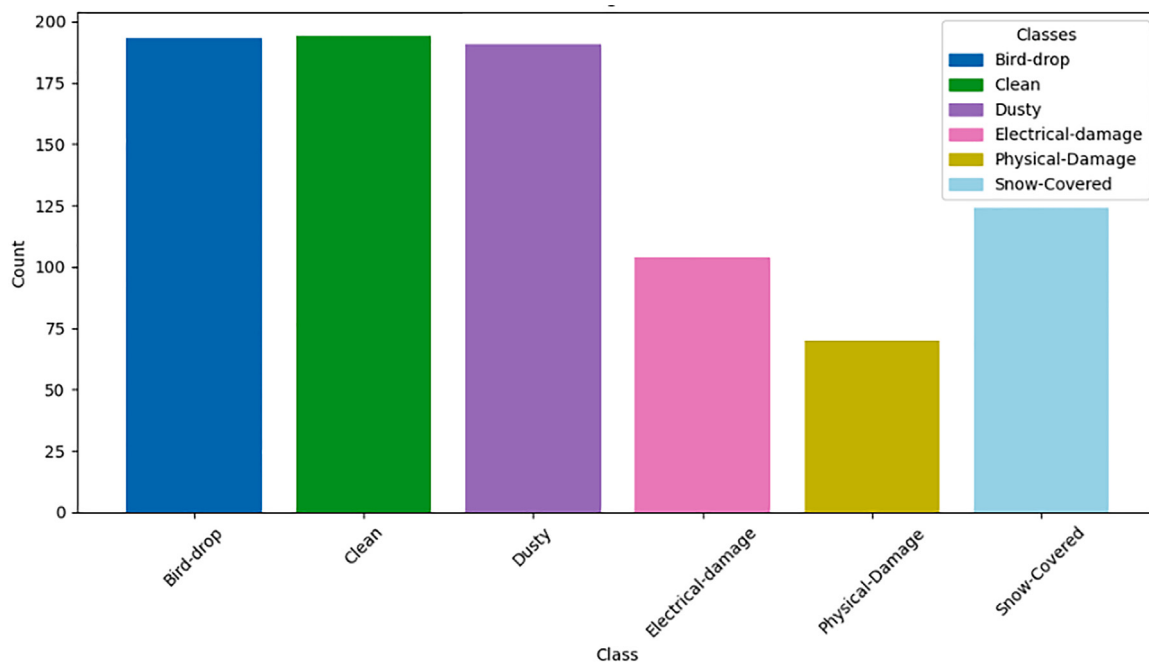


Fig. 6. The distribution of solar panel dataset categories in 6 classes — bird droppings, cleanliness, dust accumulation, electrical damage, physical damage, and snow coverage.

Optimization involves prefetching data. This complete methodology guarantees that the data is suitably prepared for model training by ensuring uniform picture sizes and pixel normalization, enhancing model performance. Furthermore, the dataset is improved by applying random rotations to the pictures and masks, augmenting the variability in the training data. This facilitates the model's ability to extrapolate more effectively to diverse orientations and angles (Mujtaba and ArifWani, 2021). Additionally, the photographs undergo random cropping and resizing at various sizes, imitating diverse views and viewpoints. This augmentation strategy enhances the model's ability to handle item size and location fluctuations within the photos, making it more robust (Wu et al., 2022).

4. Proposed models

We can find the solar panel using the U-Net model architecture for satellite image segmentation. This section introduces a proposed deep-learning model architecture for finding the panel faults.

4.1. Deep learning models

Deep learning models like U-Net, Dense-Net, MobileNetV3, VGG19, CNN, VGG16, Resnet50, InceptionV3, and a proposed InceptionV3-Net models are utilized for solar panel fault detection due to their advanced capabilities in automatically detecting and segmenting features in imagery. These models enhance the precision and efficiency of fault identification tasks, such as finding panel abnormal issues. Implementing base models enables scalable and automated surveillance of extensive solar farms, ensuring reliable operation even amidst diverse environmental conditions (Karagoz et al., 2022). Including various architectures allows for a comprehensive improvement of the fault detection process in solar panels.

4.2. U-Net model architecture

U-Net architecture is utilized to conclude the image segmentation process of solar panel (Slonimer et al., 2022; Gonthina et al., 2024). The U-Net architecture completes the segmentation operation in stage four.

Table 4
Encoder feature layers in the U-net model.

Layer name	Resolution
Block 1 Relu	64 x 64
Block 3 Relu	32 x 32
Block 6 Relu	16 x 16
Block 13 Relu	8 x 8
Block 16 Project	4 x 4

Table 5
Up-sampling blocks in the U-net decoder.

Up-sampling resolution	Number of filters
4 x 4 to 8 x 8	512
8 x 8 to 16 x 16	256
16 x 16 to 32 x 32	128
32 x 32 to 64 x 64	64

Stage 1 Encoder (Down-sampler): The encoder begins with a pre-trained MobileNetV2 model with input shape $256 \times 256 \times 3$ and the top classification layers. For feature extraction, certain layers from the MobileNetV2 model are chosen (Li et al., 2022; Li and Chen, 2024). These layers are selected to collect characteristics at various spatial resolutions in Table 4

Stage 2 Decoder (Up-sampler): The up-sample function defines a set of up-sampling blocks that are used in the construction of the decoder. Each block starts with a transposed convolution layer (Conv2DTranspose) and then optionally adds dropout, batch normalization, and ReLU activation. U-Net architecture does the job of selecting images of solar panels. The u-net design finishes the segmentation process at layer four. These up-sampling blocks are part of the up-stack list, which makes the feature maps gradually larger in Table 5.

Stage 3 Combining Encoder and Decoder: Up-sampling is integrated with skip connections. Each up-sampling block combines the feature maps from the encoder (down stack) with the up-sampled feature maps. The inclusion of this skip link aids in the preservation of intricate information. The decoder incrementally enhances the spatial resolution until it attains the target output dimensions of 128×128 pixels.

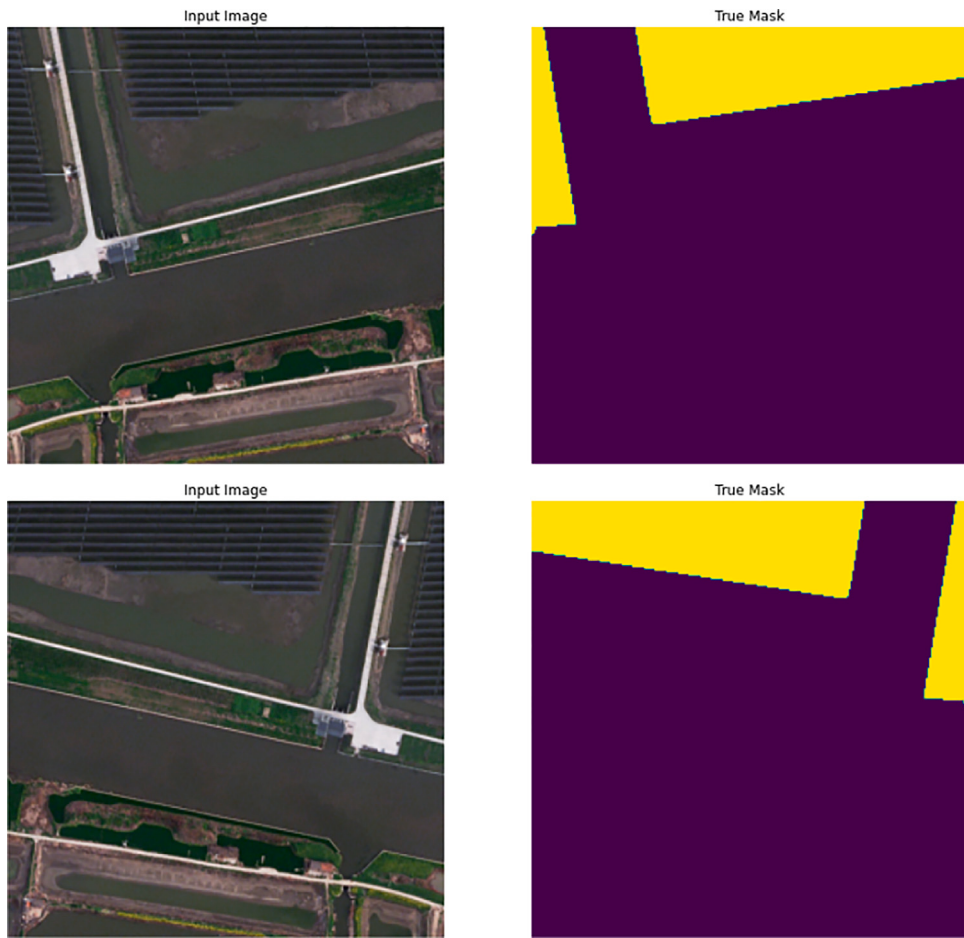


Fig. 7. Aerial images of solar panels with corresponding true mask annotations for fault detection.

Stage 4 Output layer: The final layer of the model consists of a Conv2DTranspose layer that converts the feature maps into the required output shape ($128 \times 128 \times 1$) using a sigmoid activation function (Wang and Xiao, 2023). This activation function generates binary predictions for each pixel. Fig. 8 represents the U-Net model architecture, which is structured in a flowchart format. The model consists of various layers that are sequentially connected, with some layers being concatenated with others.

The layers are labeled with Input-Layer, Sequential, and Concatenate, followed by numbers that potentially correspond to their order or level in the model. Each layer box also displays the shape of the input and output data, with dimensions specified in tuples that indicate the size of the tensors as they pass through the network. At the bottom of Fig. 8 is a layer labeled conv2d transpose 4: Conv2DTranspose, which indicates a transposed convolutional layer. This layer is used for image segmentation and generative models, where the spatial dimensions of the input are increased. By visually representing the flow and structure of the model, the diagram illustrates how data is transformed and combined as it moves through the network.

4.3. InceptionV3-Net

The range of applications and robust feature extraction capabilities of the InceptionV3 architecture make it highly suitable for identifying problems in solar panels through image analysis (Chavan and Pete, 2023a). Setting up the design is the first step in creating a model for finding faults in solar panels.

It loads the InceptionV3 base model with ImageNet weights and sets the number of fault types in Fig. 9–10. We add convolutional layers with LeakyReLU activation to avoid dying ReLU issues, 256 filters, a kernel size of (3, 3), and the same padding. It uses a sigmoid activation function to set up 64 units in the first dense layer and 128 units in the second dense layer for Squeeze-and-Excitation (SE) Blocks (Salekin et al., 2019). Thoughtfully placed residual connections improve gradient flow. Added global average pooling layer brings together spatial data in the best way possible. Two dense layers, one with 1024 units and the other with 512 units, comprise the fully connected layers. The first dense layer has LeakyReLU activation, batch normalization, and a dropout rate of 0.5. Lastly, the output layer uses a thick layer with soft-max activation for classification. It can rotate up to 15 degrees, shift up to 10% horizontally and vertically, shear transform up to 20 degrees, zoom up to 20%, flip horizontally and vertically, change brightness between 0.7 and 1.3, and fill pixels with the color of their nearby neighbors. We train the model with the Adam optimizer, which has a learning rate of 0.0001 and a loss function for category cross-entropy (Chavan and Pete, 2023b).

The proposed InceptionV3-Net architecture uses convolutional processes to apply filters that identify edges, textures, and other characteristics that suggest defects in solar panels:

- **Convolutional Layers:** In Eq. (2) σ represents a ReLU activation function, I is the input image, K^l represents the kernel of filters, and b^l is the bias term function identifying non-linear fault patterns (Hsieh et al., 2020).

$$F_{ij}^l = \sigma \left(\sum_m \sum_n I_{(i+m)(j+n)} \cdot K_{mn}^l + b^l \right) \quad (1)$$

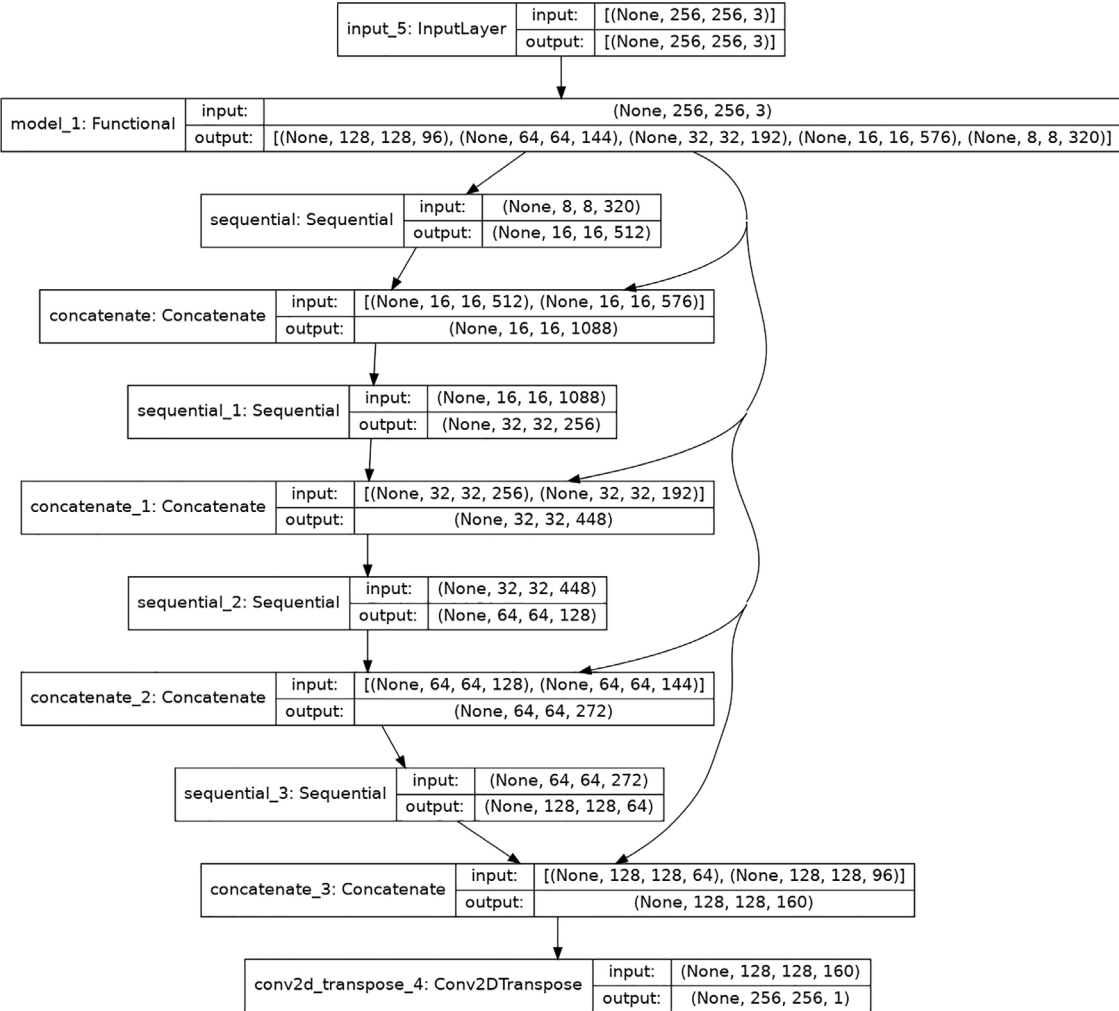


Fig. 8. U-Net Model Architecture with Layer view and input-output size.

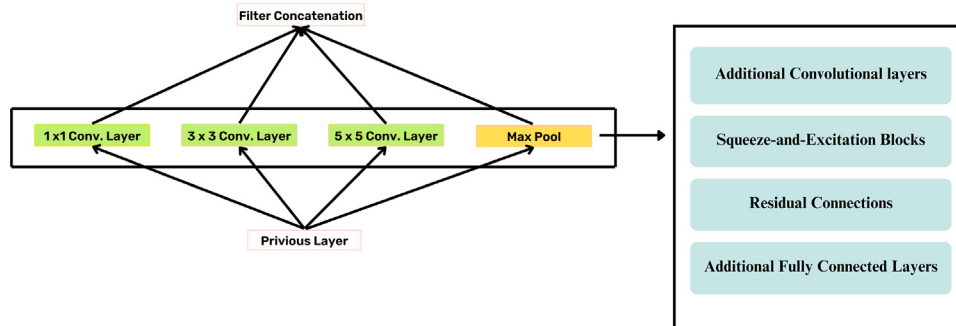


Fig. 9. Proposed InceptionV3-Net Model.

$$F_{ij}^l = \sigma \left(\sum_m \sum_n I_{(i+m)(j+n)} \cdot K_{mn}^l + b^l \right) \quad (2)$$

- **Pooling Layers:** Eq. (3) represents the reduced level of the spatial resolution to focus on prominent fault features (Rahman et al., 2021).

$$P_{ij} = \max(F_{kl}) \quad (3)$$

- **Normalization Layers:** In normalization layers, μ_B and σ_B^2 are the batch mean and variance, and γ and β are learnable parameters in Eq. (4).

$$\hat{F}_{ij}^l = \frac{F_{ij}^l - \mu_B}{\sqrt{\sigma_B^2 + \epsilon}} \cdot \gamma + \beta \quad (4)$$

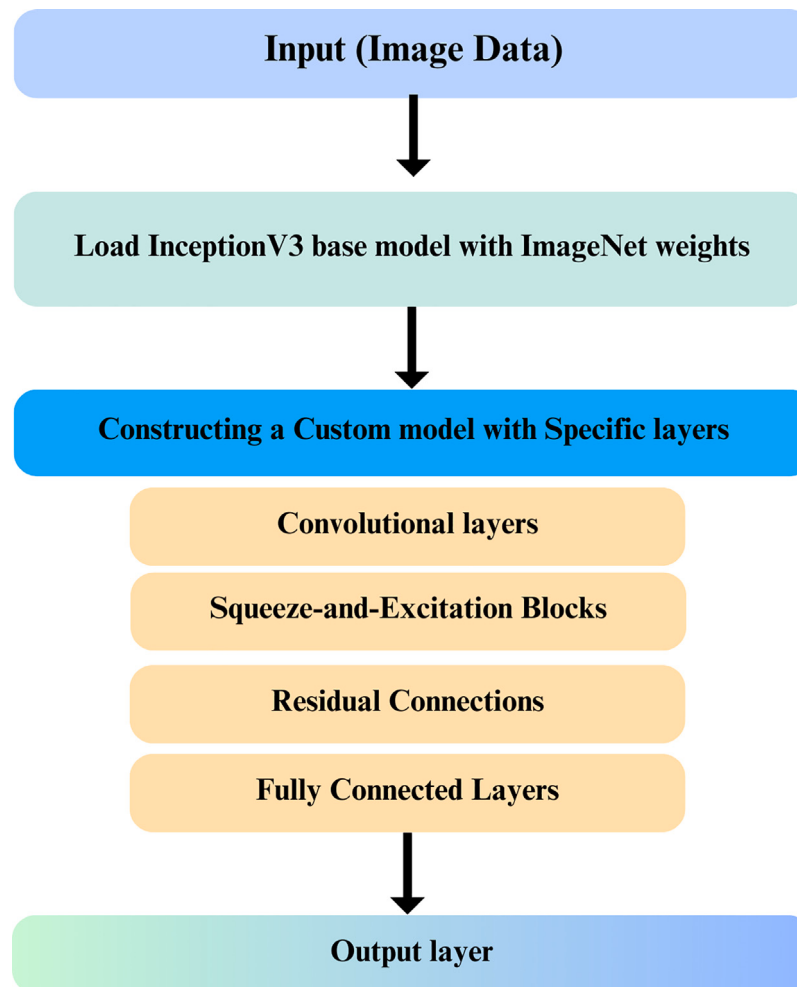


Fig. 10. Proposed InceptionV3-Net Layer Architecture.

5. Evaluation metrics

In assessing the performance of a fault detection model, particularly in applications such as solar panel fault detection, the careful selection of suitable metrics is of utmost importance. In this regard, precision in Eq. (5), recall in Eq. (6), and the F1 score (the harmonic mean of precision and recall) in Eq. (7) are remarkably appropriate metrics (Yan et al., 2022; Khan and Ali Rana, 2019). By employing precision, the model effectively detects genuine defects while reducing the occurrence of false alarms. The recall identifies many genuine defects as feasible. With context to solar panels, a high recall indicates that the model can accurately detect a diverse array of faults. F1 Score objectively evaluates the model's performance by considering precision and recall.

The Intersection over Union (IoU) in Eq. (8) is used in the analysis of satellite images for evaluating the precision of solar panel segmentation (Goyzueta et al., 2021). It measures the degree of overlap between the projected segmentation of solar panels and the ground-truth portions of solar panels in the image. In addition, the Dice coefficient measures the accuracy of segmentation models by quantifying the similarity between the predicted segmentation and the ground truth. In the context of solar panel image segmentation, it calculates the overlap between the model's prediction and actual solar panel boundaries, with a score of 1 indicating perfect agreement and 0 meaning no overlap. In Eq. (9), X represents the pixels in the predicted segmentation, and Y defines the pixels in the ground truth segmentation (Stephanie and

Sarno, 2018).

$$Precision = \frac{TP}{TP + FP} \quad (5)$$

where, TP = True Positive, FP = False Positive

$$Recall = \frac{TP}{TP + FN} \quad (6)$$

where, TP = True Positive, FN = False Negative

$$F1\ Score = 2 \times \frac{Precision \times Recall}{Precision + Recall} \quad (7)$$

$$IoU = \frac{A_o}{A_u}$$

where, IoU = Intersection over Union, A_o = Area of Solar Panel Overlap, and A_u = Area of Solar Panel Union

$$D = \frac{2|X \cap Y|}{|X| + |Y|}$$

where, D is the Dice Coefficient, $|X \cap Y|$ is the intersection, $|X|$ and $|Y|$ are the sizes of the pixel sets.

6. Segmentation model outcome

Our research paper presents outcomes of segmentation and classification models, evaluated using the formulas outlined in Section 5.

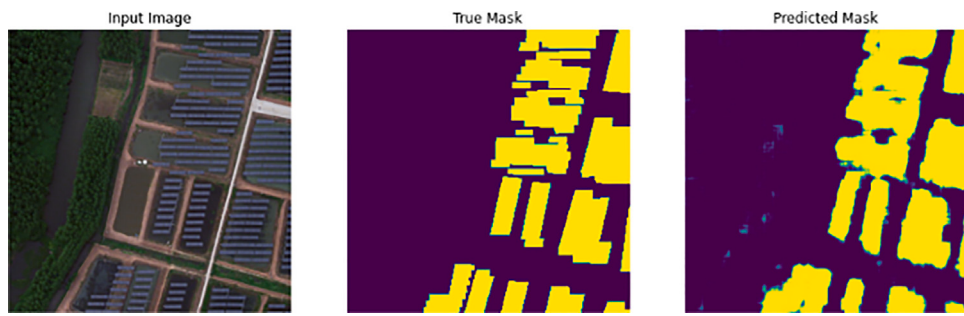


Fig. 11. Satellite image of a solar plant with true and predicted segmentation masks.

Table 6

Training performance metrics for U-net architecture on segmentation dataset. Evaluating epoch-wise loss, dice coefficient, binary accuracy, and IoU Score.

Epoch	Loss	Dice Coef	Bin Acc	IoU Score
1	0.4520	0.5480	0.7885	0.4423
2	0.1951	0.8097	0.9540	0.7323
3	0.1752	0.8236	0.9531	0.7479
4	0.1656	0.8368	0.9568	0.7641
5	0.1553	0.8433	0.9601	0.7690
6	0.1632	0.8369	0.9570	0.7657
7	0.1625	0.8391	0.9583	0.7688
8	0.1616	0.8387	0.9567	0.7685

Table 7

Validation performance metrics for U-net architecture on segmentation dataset. Evaluating epoch-wise loss, dice coefficient, binary accuracy, and IoU score.

Epoch	Loss	Dice Coef	Bin Acc	IoU score
1	0.1878	0.8108	0.9437	0.7266
2	0.1738	0.8259	0.9541	0.7517
3	0.1668	0.8324	0.9546	0.7562
4	0.1610	0.8389	0.9559	0.7668
5	0.1653	0.8345	0.9556	0.7606
6	0.1701	0.8296	0.9539	0.7537
7	0.1687	0.8317	0.9569	0.7621
8	0.1659	0.8341	0.9563	0.7631

6.1. U-Net model performance

The performance of a deep learning model over 8 training epochs shows consistent improvement in both training and validation phases in [Tables 6](#) and [7](#).

Training loss decreased from 0.4520 to 0.1616, indicating effective learning and error reduction. The Training Dice Coefficient, measuring precision in segmentation tasks in [Fig. 11](#), increased from 0.5480 to 0.8387, demonstrating enhanced predictive precision. Training Binary precision remained high and stable, suggesting consistent performance in binary classification. Similarly, model training loss decreased over time, signaling good generalization to segmented data.

The validation Dice Coefficient's upward trend, from 0.8108 to 0.8341, and high validation binary precision (starting at 0.9347 and reaching 0.9563) further underscores the model's strong generalization ability. These metrics collectively indicate a successful validation process, with the model showing decreased loss and improved precision in segmentation and binary classification tasks.

The IoU score is initially low, but there is a significant increase to 0.4423, and it continues to improve, reaching a high of 0.7631. That remains the same at 0.7631 in the later epochs, shown in [Fig. 12](#), which indicates that the segmentation and prediction of satellite images are working correctly.

A threshold value was used to evaluate the probability estimates provided by the U-Net segmentation model. It rotates through a subset of the test dataset as shown in [Fig. 13](#), represents a comparison between

the model's predictions and the actual masks of solar panels. Also highlights the U-Net model's high precision in segmenting solar panels from satellite images. The close match between the predicted and true masks. It extracts the image and true mask (ground truth) for each image, computes the model's probability prediction, and creates a binary mask using the threshold.

7. Classification model outcome

This section provides a comprehensive overview of the performance of the deep learning models implemented during the training and validation phases. The evaluation metrics of F1 scores, Recall, and Precision have been carefully calculated on the training and testing data sources to ascertain the model's effectiveness. The details of the training and testing performances are described below.

7.1. Model training performance

The analysis of the training accuracies of the various deep learning models shows that each model expresses varying degrees of effectiveness in learning from its training dataset, as shown in [Table 8](#). Dense-Net, with a training accuracy of only 21.28%, appears to have significant under-fitting, which indicates a failure to capture the underlying patterns in the solar panel faults data. Conversely, MobileNetV3 and VGG19 display moderate to good learning levels with an accuracy of around 70%–77%, indicating proper data performance without over-fitting. The CNN and VGG16 models are balanced around 80% accuracy, presenting a high level of learning but approaching the threshold where over-fitting might be a concern. Resnet50 reflects this trend as well. On the other hand, InceptionV3 and the proposed InceptionV3-Net stand out with exceptionally high training accuracies of over 90%, indicating effective learning. The proposed InceptionV3-Net model has achieved a high training accuracy of 99.01%. This raises concerns about over-fitting, as the models might have tailored themselves too closely to the training data. Potentially compromising their ability to generalize to new, unseen data. It is essential to balance effective learning with the ability to generalize, particularly in models that express incredibly high training accuracies. In comparing the training and validation datasets where all models perform well on the training data, their performance often drops when applied to the validation dataset. This suggests that the models are overfitting as they struggle to generalize their learning to unseen data. In the validation analysis, it was observed that all the models demonstrated varying performance levels. Among all the models, the proposed InceptionV3-Net has an exceptional F1 score of 0.99 and an impressive validation accuracy of around 98.34%.

The range of precision values lies between 0.20 to 0.99. InceptionV3-Net (proposed) exhibits the highest precision score of 0.99, while Dense-Net shows the lowest precision at 0.20. Across the models, recall values span from 0.20 to 0.98. Dense-Net achieves the most inadequate recall at 0.20, while InceptionV3-Net (proposed) exhibits the highest

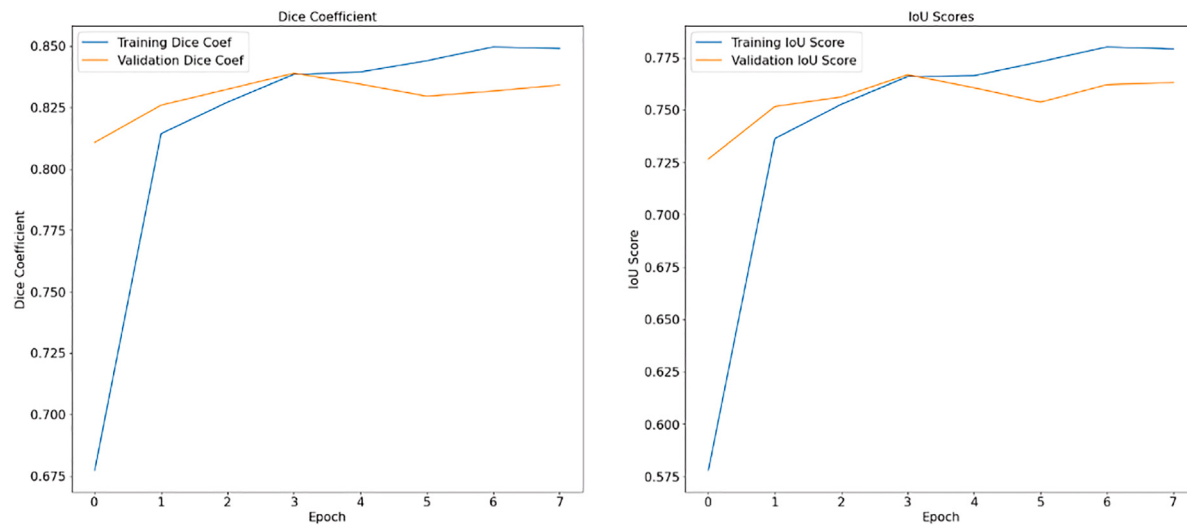


Fig. 12. Performance graph of U-Net model. The Intersection of Union (IoU) scores, with the training scores in blue and the validation scores in orange, throughout 8 epochs.

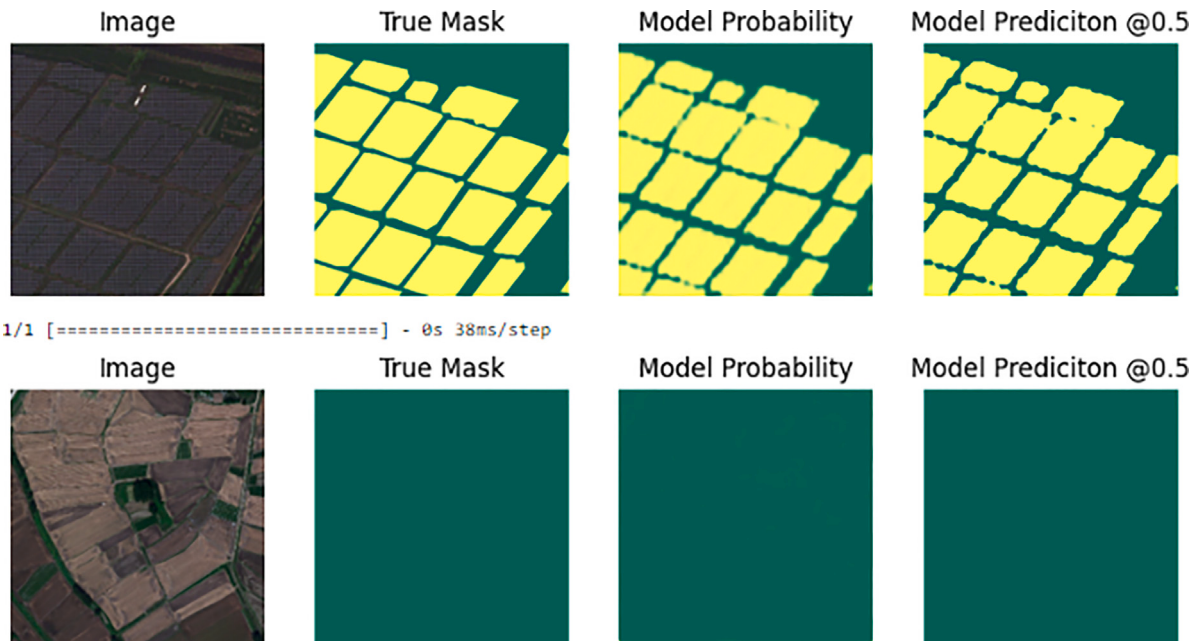


Fig. 13. Visual Evaluation of Segmentation Model. Comparing Image, True Mask, Model Probabilities, and Binary Predictions with 0.5 Threshold.

Table 8

Comparative performance metrics of various deep learning models on the solar panel fault dataset, highlighting F1 score, precision, recall, training, and validation accuracy.

Model name	F1 Score	Precision	Recall	Train accuracy	Validation accuracy
Dense-Net	0.21	0.20	0.20	21.28%	20.90%
MobileNetV3	0.70	0.71	0.70	70.71%	69.99%
VGG19	0.75	0.76	0.75	76.89%	76.01%
CNN	0.76	0.75	0.75	76.24%	74.86%
VGG16	0.81	0.81	0.80	80.16%	79.09%
Resnet50	0.80	0.80	0.80	80.19%	78.29%
InceptionV3	0.92	0.91	0.91	91.74%	89.87%
InceptionV3-Net (Proposed)	0.99	0.99	0.98	99.01%	98.34%

recall score at 0.98. The F1 Score, which represents the balance between precision and recall, shows a notable variance across the models; InceptionV3-Net (proposed) boasts the highest F1 Score of 0.99.

This analysis underscores the significance of maintaining an appropriate balance between these two factors to ensure a model's optimal performance in real-world applications.

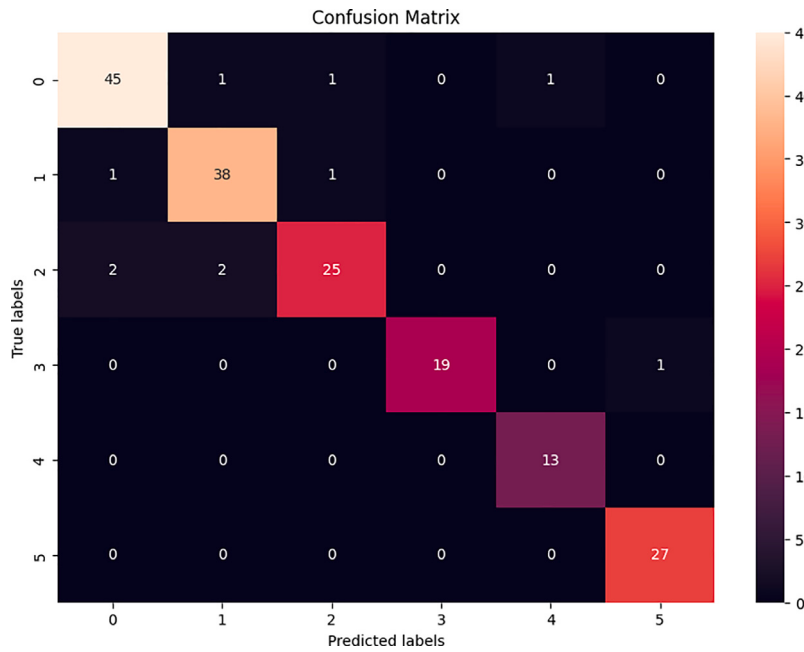


Fig. 14. Confusion matrix displaying the classification accuracy of the InceptionV3-Net, with a clear diagonal of high correct predictions.

Table 9

Comparative performance metrics of various deep learning models on the solar panel fault dataset, highlighting F1 score, precision, recall, and test accuracy for classification.

Model	F1 Score	Precision	Recall	Test accuracy
Dense-Net	0.19	0.21	0.19	21.00%
MobileNetV3	0.66	0.66	0.66	70.04%
VGG19	0.79	0.76	0.78	77.00%
CNN	0.75	0.77	0.75	79.40%
VGG16	0.79	0.87	0.80	80.00%
Resnet50	0.81	0.81	0.81	80.79%
InceptionV3	0.91	0.92	0.90	90.19%
InceptionV3-Net (Proposed)	0.94	0.94	0.94	94.35%

7.2. Model testing performance

The test accuracies of the models exhibit varying abilities to generalize to new, unseen data. This indicates a model's real-world performance, reflecting how well the model can apply the knowledge it has gained to new situations and scenarios. The model with the lowest test accuracy is Dense-Net, with a score of 21.00% in Table 9. This suggests that there is a significant need for improvement in terms of generalization. MobileNetV3 performs moderately well with a test accuracy of 70.04%, indicating that it can handle new data reasonably well.

VGG19 shows a better ability to learn, with a test accuracy of 77.00%, suggesting that it has learned patterns widely applicable beyond the training set. The CNN model displays an excellent ability to adapt to new data, with a test accuracy of 79.40%. VGG16's test accuracy of 80.00% is commendable, indicating that it learns well and effectively applies these leanings to novel scenarios. A modified version of the VGG16 model achieved a test accuracy of 80.05% by adding dense layers of different unit sizes (1024, 512, 256, and 128) and using the Rectified Linear Unit (ReLU) activation algorithm. After each layer, a dropout layer with a specific dropout rate (0.5, 0.4, 0.3, and 0.2) was added. In comparison, the base model of VGG16 and the modified VGG16 model showed slight improvements. Resnet50, with a test accuracy of 80.79%, slightly surpasses VGG16, indicating a slightly

better ability to apply its knowledge to unseen data. Fig. 14 visually represents the confusion matrix of InceptionV3-Net performance across six classes. The high diagonal values indicate correct classifications and the matrix suggests a strong predictive ability, with certain classes showing higher instances of accurate predictions.

The most imposing models are InceptionV3 and the proposed InceptionV3-Net, with test accuracies of 90.19% and 94.35%, respectively. These high scores indicate exceptional adaptability, demonstrating that these models can recognize complex patterns and apply them effectively to new situations. This is particularly noteworthy for InceptionV3-Net, which balances a high learning capability with excellent adaptability, as reflected in its performance. In the context of F1 scores, the analysis reveals that Dense-Net displays the lowest F1 Score of 0.19, while MobileNetV3, VGG19, CNN, VGG16, and Resnet50 exhibit moderate performance. When comparing the precision and recall abilities of the tested models, InceptionV3 and InceptionV3-Net (Proposed) stand out as they demonstrate high precision scores of 0.92 and 0.94, respectively.

7.3. Discussion

The U-Net model has shown significant improvement in solar plant satellite image segmentation. The metrics indicate reduced training loss and increased training and testing Dice Coefficient, binary precision, and intersection over union (IoU) scores. These observations suggest that the U-Net model is highly efficient and accurate in segmenting solar plant images, making it a reliable and effective tool for precise image segmentation tasks.

In the context of solar panel fault detection, the performance of the models varies significantly, as indicated by their F1 Score, precision, and recall. Dense-Net is a notable under-performer, reflected in its low F1 Score of 0.19, Precision of 0.21, and Recall of 0.19, aligning with its poor training, validation, and test accuracies of around 21%. This suggests substantial difficulties in learning and generalizing. In contrast, MobileNetV3 exhibits a moderate performance level with balanced metrics: an F1 Score of 0.66 and both precision and recall at 0.66. It corresponds to its closely aligned training, validation, and test



Fig. 15. Proposed InceptionV3-Net model predictions on solar panel cleanliness, showcasing high accuracy in distinguishing between clean and dusty panels.

accuracies of around 70%, indicating a well-balanced model without severe over-fitting or under-fitting.

On the other hand, VGG19 and CNN models demonstrate more robust performance. VGG19 has an F1 score of 0.79, precision of 0.76, and recall of 0.78, while CNN shows an F1 Score of 0.75, precision of 0.77, and recall of 0.75. Both models exhibit slightly higher test accuracies than their training accuracies, suggesting practical tuning and strong generalization capabilities. VGG16 and Resnet50 also perform well, with VGG16 recording an F1 score of 0.79, precision of 0.87, and recall of 0.80, and Resnet50 showing consistently high values with an F1 Score, precision, and recall all at 0.81. These metrics indicate reliable and precise fault detection abilities. The InceptionV3 and proposed InceptionV3-Net models stand out with their exceptional performance in InceptionV3 with an F1 score of 0.91, precision of 0.92, and recall of 0.90, and InceptionV3-Net with all metrics at 0.94. Despite a slight drop in test accuracies, these high values underscore their exceptional precision and recall in fault detection, making them highly suitable for practical solar panel fault detection applications.

From the previous background studies, the effectiveness of deep learning models in fault detection and segmentation tasks. Recent studies highlight the significant improvement in performance metrics such as Dice Coefficient and IoU scores when using advanced segmentation models such as U-Net. For instance, [Adhya et al. \(2022\)](#) demonstrated that selective machine learning techniques could enhance PV array fault diagnosis, improving the robustness and reliability of the detection systems. This aligns with our findings of U-Net's efficiency and accuracy in segmenting solar plant images. Additionally, [Pamungkas et al. \(2023\)](#) have shown that architectures similar to ResNet and VGG are robust in handling diverse classification tasks under varying conditions. The observations of VGG19 and Resnet50's strong generalization capabilities and reliable performance metrics. These models consistently exhibit high F1 scores, precision, and recall, reinforcing their suitability for precise fault detection tasks. In terms of InceptionV3 architecture, [Li and Chen \(2024\)](#) validate the high performance of this model in

image recognition tasks. Their work supports the exceptional results of our proposed InceptionV3-Net model, which achieved high accuracy, precision, and recall in practical solar panel fault detection scenarios.

The precise identification and categorization of faults is facilitated by the proposed InceptionV3-Net model. [Fig. 15](#) presents the model's predictions on the cleanliness of solar panels, distinguishing between clean and dusty panels with high accuracy with validates the InceptionV3-Net model in real-world scenarios. It enables targeted and efficient corrective actions by minimizing downtime and maximizing the performance of solar panels. The fault detection systems ensure that specific issues impacting power generation, such as shading, module degradation, or electrical failures, can be promptly addressed. As a result, the enhanced accuracy of this model positively contributes to improving operational efficiency, increasing energy yield, and extending the lifespan of solar installations.

8. Comparative analysis

The findings of this study demonstrate that the proposed InceptionV3-Net model achieves superior accuracy in solar panel fault detection. Unlike previous models by [Adhya et al. \(2022\)](#) and [Pamungkas et al. \(2023\)](#), which lack advanced segmentation and hybrid modeling capabilities, the InceptionV3-Net effectively integrates these techniques, significantly enhancing fault detection accuracy. Additionally, it addresses the computational efficiency issues noted in [Li and Chen \(2024\)](#) and fully leverages data augmentation to improve robustness and reduce overfitting, as highlighted by [Wu et al. \(2022\)](#). In contrast to [Slonimer et al. \(2022\)](#) and [Li et al. \(2022\)](#), who focused on hybrid models and efficiency without comprehensive data augmentation, the InceptionV3-Net combines all these critical aspects. [Rahman et al. \(2021\)](#) emphasized hybrid models but lacked adequate segmentation and augmentation which is shown in [Table 10](#). By integrating these essential components, the InceptionV3-Net not only improves

Table 10
Comparative analysis of deep learning models for solar panel fault detection.

Authors	Fault predict	Img. Segment	Hybrid model	Augmentation	Comp. Eff.
Adhya et al. (2022)	✓	✗	✗	✗	✓
Pamungkas et al. (2023)	✓	✗	✗	✗	✓
Li and Chen (2024)	✓	✓	✗	✓	✗
Wu et al. (2022)	✓	✓	✗	✓	✓
Slonimer et al. (2022)	✓	✓	✓	✗	✓
Li et al. (2022)	✓	✓	✗	✗	✗
Rahman et al. (2021)	✓	✗	✓	✗	✓
Proposed InceptionV3-Net	✓	✓	✓	✓	✓

fault detection accuracy but also enhances operational efficiency and reliability.

9. Conclusion

In this research, we present a novel InceptionV3-Net model, significantly improving solar panel fault detection. Initially, aerial satellite images are processed using the U-net model architecture with a $256 \times 256 \times 3$ input shape, undergoing three stages: decoding the input, combining encoding and decoding, and generating the output. The InceptionV3-Net architecture employs the InceptionV3 base with ImageNet weights, enhanced by convolutional layers, Squeeze-and-Excitation (SE) blocks, residual connections, and global average pooling. The model includes two dense layers with LeakyReLU and batch normalization, ending with a Soft-Max output layer. It also utilizes data augmentation techniques such as rotation, shift, shear, zoom, and brightness adjustments. The model is trained using the Adam optimizer with a learning rate of 0.0001 and categorical cross-entropy loss. The InceptionV3-Net model expresses exceptional performance by achieving a validation accuracy of 98.34%, test accuracy of 94.35%, an F1 Score of 0.94, a precision of 0.94, and a recall of 0.94 outperforming other researcher's works. Future work could address several open scopes to further improvement in the InceptionV3-Net model's capabilities. Applying the model to other renewable energy systems, such as wind turbines or hydroelectric plants, would test its versatility. Further optimization of the model for real-time fault detection could be outlined as future work to improve its practical utility.

Funding

This research is funded by the Researchers Supporting Project Number (RSPD2024R1027), King Saud University, Riyadh, Saudi Arabia.

CRediT authorship contribution statement

Rifat Al Mamun Rudro: Writing – original draft, Conceptualization. **Kamruddin Nur:** Formal analysis, Data curation. **Md. Faruk Abdullah Al Sohan:** Methodology, Investigation. **M.F. Mridha:** Validation, Supervision. **Sultan Alfarhood:** Writing – review & editing, Visualization, Validation. **Mejdl Safran:** Resources, Project administration, Funding acquisition. **Karthick Kanagarathinam:** Supervision, Formal analysis.

Declaration of competing interest

The authors declare no conflict of interest.

Data availability

Data will be made available on request.

Acknowledgments

The authors extend their appreciation to King Saud University for funding this research through Researchers Supporting Project Number (RSPD2024R1027), King Saud University, Riyadh, Saudi Arabia.

References

- Adhya, D., Chatterjee, S., Chakraborty, A.K., 2022. Performance assessment of selective machine learning techniques for improved PV array fault diagnosis. *Sustain. Energy Grids Netw.* 29 (100582), 100582.
- Alsaafseh, M., Abdel-Qader, I., Bazuin, B., Alsafasfeh, Q., Su, W., 2018a. Unsupervised fault detection and analysis for large photovoltaic systems using drones and machine vision. *Energies* 11 (9), 2252.
- Alsaafseh, M., Abdel-Qader, I., Bazuin, B., Alsafasfeh, Q., Su, W., 2018b. Unsupervised fault detection and analysis for large photovoltaic systems using drones and machine vision. *Energies* 11 (9), 2252.
- Anon, 2021. Deep learning methods for solar fault detection and classification: A review. *Inf. Sci. Lett.* 10 (2), 323–331.
- Badr, M.M., Hamad, M.S., Abdel-Khalik, A.S., Hamdy, R.A., Ahmed, S., Hamdan, E., 2021. Fault identification of photovoltaic array based on machine learning classifiers. *IEEE Access* 9, 159113–159132.
- Bemposta Rosende, S., Sánchez-Soriano, J., Gómez Muñoz, C.Q., Fernández Andrés, J., 2020. Remote management architecture of UAV fleets for maintenance, surveillance, and security tasks in solar power plants. *Energies* 13 (21), 5712.
- Chavan, R., Pete, D., 2023a. Classification of retinal fundus images using VGG16 and inception V3. In: 2023 14th International Conference on Computing Communication and Networking Technologies. ICCCNT, pp. 1–5. <http://dx.doi.org/10.1109/ICCCNT56998.2023.10306593>.
- Chavan, R., Pete, D., 2023b. Classification of retinal fundus images using VGG16 and inception V3. In: 2023 14th International Conference on Computing Communication and Networking Technologies. ICCCNT, pp. 1–5. <http://dx.doi.org/10.1109/ICCCNT56998.2023.10306593>.
- Chen, X., Karin, T., Libby, C., Deceglie, M., Hacke, P., Silverman, T.J., Jain, A., 2023. Automatic crack segmentation and feature extraction in electroluminescence images of solar modules. *IEEE J. Photovolt.* 13 (3), 334–342.
- Dhanraj, J.A., Mostafaipour, A., Velmurugan, K., Techato, K., Chaurasiya, P.K., Solomon, J.M., Gopalan, A., Phoungthong, K., 2021. An effective evaluation on fault detection in solar panels. *Energies* 14 (22), 7770.
- Duranay, Z.B., 2023. Fault detection in solar energy systems: A deep learning approach. *Electronics (Basel)* 12 (21), 4397.
- Fazai, R., Abodayeh, K., Mansouri, M., Trabelsi, M., Nounou, H., Nounou, M., Georgiou, G.E., 2019. Machine learning-based statistical testing hypothesis for fault detection in photovoltaic systems. *Sol. Energy* 190, 405–413.
- García, E., Quiles, E., Correcher, A., Morant, F., 2022. Predictive diagnosis based on predictor symptoms for isolated photovoltaic systems using MPPT charge regulators. *Sensors (Basel)* 22 (20), 7819.
- Gonthina, N., Adunuri, S., Mateti, R., Allampalli, S.S., Narasimha Prasad, L.V., 2024. Accurate semantic segmentation of aerial imagery using attention res-U-net architecture. In: 2024 International Conference on Emerging Smart Computing and Informatics. ESCI, pp. 1–5. <http://dx.doi.org/10.1109/ESCI59607.2024.10497287>.
- Goyzueta, C.A.R., De la Cruz, J.E.C., Machaca, W.A.M., 2021. Integration of U-Net, ResU-Net and DeepLab architectures with intersection over union metric for cells nuclei image segmentation. In: 2021 IEEE Engineering International Research Conference. EIRCON, pp. 1–4. <http://dx.doi.org/10.1109/EIRCON52903.2021.9613150>.
- Henry, C., Poudel, S., Lee, S.-W., Jeong, H., 2020. Automatic detection system of deteriorated PV modules using drone with thermal camera. *Appl. Sci. (Basel)* 10 (11), 3802.
- Hou, J., Ling, Y., Yujun, L., 2021. Multi-resolution dataset for photovoltaic panel segmentation from satellite and aerial imagery. <http://dx.doi.org/10.5281/ZENODO.5171712>, URL <https://zenodo.org/record/5171712>.
- Hsieh, Y.-C., Chin, C.-L., Wei, C.-S., Chen, I.-M., Yeh, P.-Y., Tseng, R.-J., 2020. Combining VGG16, mask R-CNN and inception V3 to identify the benign and malignant of breast microcalcification clusters. In: 2020 International Conference on Fuzzy Theory and Its Applications. IFUZZY, pp. 1–4. <http://dx.doi.org/10.1109/IFUZZY50310.2020.9297809>.
- Hu, A., Levis, S., Mehl, G.A., Han, W., Washington, W.M., Oleson, K.W., van Ruijven, B.J., He, M., Strand, W.G., 2016. Impact of solar panels on global climate. *Nat. Clim. Chang.* 6 (3), 290–294.

- Karagoz, M.A., Karaboga, D., Akay, B., Basturk, A., Nalbantoglu, O.U., 2022. Deep learning based steatosis quantification of liver histopathology images using unsupervised feature extraction. In: 2022 2nd International Conference on Computing and Machine Intelligence. ICMI, pp. 1–4. <http://dx.doi.org/10.1109/ICMI55296.2022.9873795>.
- Kellil, N., Aissat, A., Mellit, A., 2023. Fault diagnosis of photovoltaic modules using deep neural networks and infrared images under Algerian climatic conditions. *Energy (Oxf.)* 263 (125902), 125902.
- Khan, M.I., Al Huneidi, D.I., Asfand, F., Al-Ghamdi, S.G., 2023. Climate change implications for optimal sizing of residential rooftop solar photovoltaic systems in Qatar. *Sustainability* 15 (24), 16815.
- Khan, S.A., Ali Rana, Z., 2019. Evaluating performance of software defect prediction Models Using Area under precision-recall curve (AUC-PR). In: 2019 2nd International Conference on Advancements in Computational Sciences. ICACS, pp. 1–6. <http://dx.doi.org/10.23919/ICACS.2019.8689135>.
- Li, D., Chen, X., 2024. Lane line segmentation based on comparative analysis of three convolutional neural networks SegNet, U-Net and attention-U-Net. In: 2024 IEEE 2nd International Conference on Control, Electronics and Computer Technology. ICCECT, pp. 1002–1009. <http://dx.doi.org/10.1109/ICCECT60629.2024.10545939>.
- Li, J., Shi, L., Fu, H., 2024. Multi-objective short-term optimal dispatching of cascade hydro wind solar thermal hybrid generation system with pumped storage hydropower. *Energies* 17 (1), <http://dx.doi.org/10.3390/en17010098>, URL <https://www.mdpi.com/1996-1073/17/1/98>.
- Li, X., Yang, X., Li, X., Lu, S., Ye, Y., Ban, Y., 2022. GCDB-UNet: A novel robust cloud detection approach for remote sensing images. *Knowl.-Based Syst.* 238 (107890), 107890.
- Li, D., Zhu, D., Tao, T., Qu, J., 2023. Power generation prediction for photovoltaic system of hose-drawn traveler based on machine learning models. *Processes (Basel)* 12 (1), 39.
- Liu, W., Huo, H., Ji, L., Zhao, Y., Liu, X., Li, J., 2023. A method for extracting photovoltaic panels from high-resolution optical remote sensing images guided by prior knowledge. *Remote Sens. (Basel)* 16 (1), 9.
- Mujtaba, T., ArifWani, M., 2021. Photovoltaic solar array mapping using supervised fully convolutional neural networks. In: 2021 8th International Conference on Computing for Sustainable Global Development (INDIACom). pp. 98–103.
- Naveen Venkatesh, S., Sugumaran, V., 2021. Fault detection in aerial images of photovoltaic modules based on deep learning. *IOP Conf. Ser. Mater. Sci. Eng.* 1012 (1), 012030.
- Ou-Yang, L., Ren, Y., 2009. The development of wind-solar energy systems in China. In: 2009 International Conference on Energy and Environment Technology. Vol. 3, pp. 626–627. <http://dx.doi.org/10.1109/ICEET.2009.619>.
- Pamungkas, R.F., Utama, I.B.K.Y., Jang, Y.M., 2023. A novel approach for efficient solar panel fault classification using coupled UDenseNet. *Sensors (Basel)* 23 (10).
- Rahman, M.R., Tabassum, S., Haque, E., Nishat, M.M., Faisal, F., Hossain, E., 2021. CNN-based deep learning approach for micro-crack detection of solar panels. In: 2021 3rd International Conference on Sustainable Technologies for Industry 4.0. STI, pp. 1–6. <http://dx.doi.org/10.1109/STI53101.2021.9732592>.
- Ramaneti, K., Kakani, P., Prakash, S., 2021. Improving solar panel efficiency by solar tracking and tilt angle optimization with deep learning. In: 2021 5th International Conference on Smart Grid and Smart Cities. ICSGSC, pp. 102–106. <http://dx.doi.org/10.1109/ICSGSC52434.2021.9490485>.
- Rao, S., Spanias, A., Tepepedelenlioglu, C., 2019. Solar array fault detection using neural networks. In: 2019 IEEE International Conference on Industrial Cyber Physical Systems (ICPS). IEEE.
- Salekin, M.S., Babaeian Jelodar, A., Kushol, R., 2019. Cooking state recognition from images using inception architecture. In: 2019 International Conference on Robotics, Electrical and Signal Processing Techniques. ICREST, pp. 163–168. <http://dx.doi.org/10.1109/ICREST.2019.8644262>.
- Sharma, A., Sharma, M., 2017. Power & energy optimization in solar photovoltaic and concentrated solar power systems. In: 2017 IEEE PES Asia-Pacific Power and Energy Engineering Conference. APPEEC, pp. 1–6. <http://dx.doi.org/10.1109/APPEEC.2017.8308973>.
- Slonimer, A.L., Cote, M., Marques, T.P., Rezvanifar, A., Dosso, S.E., Albu, A.B., Ersahin, K., Mudge, T., Gauthier, S., 2022. Instance segmentation of herring and salmon schools in acoustic echograms using a hybrid U-net. In: 2022 19th Conference on Robots and Vision (CRV). IEEE.
- Snegirev, D.A., Eroshenko, S.A., Valiev, R.T., Khalyasmaa, A.I., 2017. Algorithmic realization of short-term solar power plant output forecasting. In: 2017 IEEE II International Conference on Control in Technical Systems. CTS, pp. 228–231. <http://dx.doi.org/10.1109/CTSYS.2017.8109532>.
- Sridharan, N.V., Sugumaran, V., 2021. Visual fault detection in photovoltaic modules using decision tree algorithms with deep learning features. *Energy Sources Recovery Util. Environ. Eff.* 1–17.
- Stephanie, C., Sarno, R., 2018. Detecting business process anomaly using graph similarity based on dice coefficient, vertex ranking and spearman method. In: 2018 International Seminar on Application for Technology of Information and Communication. pp. 171–176. <http://dx.doi.org/10.1109/ISEMANTIC.2018.8549830>.
- Wang, Y., Xiao, B., 2023. Convection-UNet: A deep convolutional neural network for convection detection based on the geo high-speed imager of fengyun-4B. In: 2023 International Conference on Pattern Recognition, Machine Vision and Intelligent Algorithms. PRMVIA, pp. 163–168. <http://dx.doi.org/10.1109/PRMVIA58252.2023.00033>.
- Wu, Y.-N., Liu, D., Liu, X.-C., 2022. Solar filament segmentation based on AA-UNet. In: 2022 International Conference on Automation, Robotics and Computer Engineering (ICARCE). IEEE.
- Yan, B.-C., Wang, H.-W., Jiang, S.-W.F., Chao, F.-A., Chen, B., 2022. Maximum F1-score training for end-to-end mispronunciation detection and diagnosis of L2 english speech. In: 2022 IEEE International Conference on Multimedia and Expo. ICME, pp. 1–5. <http://dx.doi.org/10.1109/ICME52920.2022.9858931>.